Automatic Multichannel Volcano-Seismic Classification Using Machine Learning and EMD

Pablo Lara, C. Alexandre Rolim Fernandes, Adolfo Inza, Jerome I. Mars,
Jean-Philippe Métaxian, Mauro Dalla Mura, Marielle Malfante

HAL Id: hal-02535142
https://hal.science/hal-02535142

Submitted on 7 Apr 2020

Automatic Multichannel Volcano-Seismic Classification Using Machine Learning and EMD

Pablo E. Lara, C. Alexandre R. Fernandes, Adolfo Inza,
Jérôme I. Mars, Jean-Philippe Métaxian, Mauro Dalla Mura, Marielle Malfante

Abstract—This article proposes the design of an automatic classifier using the empirical mode decomposition (EMD) along with machine learning techniques for identifying the five most important types of events of the Ubinas volcano, the most active volcano in Peru. The proposed method uses attributes from temporal, spectral and cepstral domains, extracted from the EMD of the signals, as well as a set of pre-processing and instrument correction techniques. Due to the fact that multichannel sensors are currently being installed in seismic networks worldwide, the proposed approach uses a multichannel sensor to perform the classification, contrary to the usual approach of the literature of using a single channel. The presented method is scalable to use data from multiple stations with one or more channels. The principal component analysis (PCA) method is applied to reduce the dimensionality of the feature vector and the supervised classification is carried out by means of several machine learning algorithms, the support vector machine (SVM) providing the best results. The presented investigation was tested with a large database that has a considerable number of explosion events, measured at the Ubinas volcano, located in Arequipa, Peru. The proposed classification system achieved a success rate of more than 90%.

I. INTRODUCTION

The recent eruption of the *Volcan de Fuego* volcano (June 2018, Guatemala) showed the catastrophic effects of a small volcanic eruption. Cataloged with an index of 3 on the Volcanic Explosive Index (VEI 3) scale, this eruption destroyed a large amount of infrastructure and killed more than 300 people. Volcanic activities have been a latent threat to humans since the existence of humanity. Indeed, many cities and towns are located in areas of impact and high risk, such as the city of Arequipa and the valleys of the volcanic chain in southern Peru, and the city of Yogyakarta, Indonesia, close to the Merapi volcano [1].

The magma interacts with the surrounding environment during its way to the crater in a system of ducts, causing disturbances when it is near the surface and generating seismic activity that can be observed by the seismic sensors. When the volcanic seismicity increases, the probability of eruption gets high. Although it can be just a mild activity, it can also be a catastrophic eruption. This question can be elucidated by analyzing seismic time series, through the classification of volcano-seismic patterns. The volcano-seismic signals can be categorized into 5 main classes [2], [3]: Long Period (LP), Tremors (TR), Explosion (EX), Volcano-Tectonic (VT) and Hybrid (HB).

Thanks to the advance of technology, there are currently more and more volcanoes monitored with seismic networks. A large amount of seismic data is observed worldwide and the analysis of these time series can be used to predict or detect the eruptive state of volcanoes. However, in many places, this data is still classified manually, which can lead to errors or delays in event detection.

Many works proposed systems for classifying seismic signals, such as [4], which uses time-frequency representations to classify local earthquakes, far earthquakes and chemical explosions, and [5], that uses power spectral density (PSD) spectrograms to classify urban seismic noise. Moreover, [6] used neural networks to classify earthquakes and quarry blasts, while [7] presented a method for automatic identification of noisy seismic events. Also, new techniques are found in the literature for classifying seismic signals with machine learning models, such as the use of the cepstral domain with support vector machine (SVM) in [8] or with Hidden Markov Model (HMM) in [9]. Besides, a three-channel seismic signal decomposition using wavelets with kernel ridge regression is presented in [10].

In the case of volcano-seismic signals, machine learning classification is also a promising method. For instance, the works [11]–[13] use time-frequency features with neural networks, while [14]–[16] use HMM for classifying volcano-seismic signals. In addition, the work [17] uses wavelet decomposition as part of the classifier and [18] uses attributes in the temporal, spectral and cepstral domains for the extraction of attributes, along with the SVM classifier.

The present work presents the design of a classifier for identifying the aforementioned five most important types of events a volcano, with a methodology that can be easily implemented in monitoring centers in real time. The objective is to automatically classify volcano-seismic signals and generate a catalog of time series of this type of signals, with the aim of finding a seismic pattern associated with the magma behavior.

The empirical mode decomposition (EMD) [19] is used to include more physical contrast in the machine learning algorithm, as the EMD is a natural adaptive decomposition method that is well-suited for non-stationary signals, as in the case of the seismic signals. The basic idea is to decompose multichannel seismic signals into components that occupy different frequency bands, called intrinsic mode functions (IMFs). In the present article, the natural characteristics of the IMFs are exploited to generate the feature vector using attributes in temporal, spectral and cepstral domains, in order to obtain a better representation of the different types of signals to be classified.

Contrarily to the usual approach of the literature of using only a single channel, the proposed approach makes use of

a multichannel triaxial sensor to perform the classification. Indeed, apart from the vertical channel, the east and north channels are also considered. In order to clarify the importance of the use multichannel sensors, let us consider that a seismic signal is recorded by a vertical single-channel sensor. This recorded signal is, in fact, the projection of the seismic wave in the vertical channel. In addition, multichannel sensors allow capturing all the information of the seismic wave-front caused by the magmatic activity, unlike single-channel sensors, which neglects some parts of the wave-front.

This kind of triaxial sensors is currently being installed in seismic networks worldwide. The presented methodology is scalable to use data from multiple stations with one or more components, since our database includes data collected simultaneously in more than one seismic station. Logically, with more information added by multiples sensors and channels, the efficiency of the result is improved. The presented classification system also proposes to perform of a set of processing and instrument correction operations in the original seismic signals captured by the sensors (signal conditioning), in order to transform the signals of each channel in meters per seconds [20].

The proposed automatic classification system can be summarized in the following steps. Firstly, a signal conditioning is performed on the seismic signals, including offset elimination, instrumental correction, among other operations. The EMD is then calculated, with the 3 most significant IMFs being selected. Next, the extraction of the attributes in temporal, spectral and cepstral domains is performed. After, the principal component analysis (PCA) method is applied to reduce the dimensionality of the feature vector. Finally, the supervised classification is carried out by means of several machine learning techniques.

This research is developed with a large database collected from two stations of the Ubinas volcano, located 70 km northeast of the city of Arequipa, in Peru. The data catalog was made by experts of the National Volcanological Center of the Geophysical Institute of Peru (IGP). The catalog of the Ubinas volcano showed, in the last years, a high number of volcano-seismic events, half a thousand events per day, which represents a difficult job for the volcanologist experts. A relevant characteristic of the database is its relatively high number of explosion events, when compared with databases of other works.

The main original contributions of this work can be summarized as follows: (i) the inclusion of a multichannel sensor and data from two seismic stations to model the behavior of the volcano, contrary to previous works that use only a single channel, (ii) the use of instrumental correction in order to make the volcanic classifier independent of the type of sensors used and to give to the energy of the signals a physical sense, (iii) the use of the EMD along with machine learning to classify the events of a volcano, and (iv) the use of database with a high number of explosion events, which can be considered one of the most important events to be detected. Moreover, the simulation showed an excellent performance of the proposed classifier when compared with other approaches. Indeed, the proposed classification system achieved a success rate of more than 90%, when the SVM technique is used.

The rest of the present work is organized as follows. Section 2 describes the database and the seismic acquisition system of the Ubinas volcano. Section 3 presents the methodology of the proposed automatic classifier, including all the aforementioned steps. In Section 4, the numerical results of the investigation are presented. Finally, Section 5 summarizes the main conclusions and perspectives of future works.

II. Ubinas Database and Acquisition System

In this section, the database and the acquisition system of the Ubinas volcano, in the city of Arequipa, Peru, are presented. The seismic database was built by experts of the National Volcanological Center of the IGP.

A. Ubinas Volcano

The Ubinas volcano (16 22 'S, 70 54' W, altitude 5672 m) began to erupt on March 25, 2006, after almost 40 years of inactivity. Located in the Central Volcanic Zone (CVZ, south of Peru), the Ubinas volcano is an active andesitic stratovolcano truncated in the upper part by a caldera with a diameter of 600m. The caldera floor is a flat area approximately 5,100 m above sea level. The active crater is located in the southern section and the bottom is 300 m below the floor of the caldera. Ubinas is considered the most active Peruvian volcano during the last 500 years, threatening 3,500 people living on the edge of the Ubinas Valley. The city of Arequipa, located 60 km away from this volcano, has been affected several times since 2006 due to the ash emissions [21].

B. Description of the Volcano Classes

Since the eruption of the Ubinas volcano in 2006, a large number and variety of types of waveforms have been generated, as presented in the literature [22]–[24]. These varieties of waveforms are associated with the behavior of magma, whose physical and chemical effects change depending on the trajectory and the environment it encounters on its route to the crater. The five main types of volcano-seismic events are the following:

1) Volcano-Tectonic (VT): They are associated with the breakage of rocks due to the high pressure produced by the magma and can even activate internal faults in the volcanic building.
2) Long Period (LP): They correspond to the impact of the fluids moving in the volcanic system or interacting with the hydrothermal system.
3) Hybrids (HB): They are caused by fluids in the blocked ducts, which produce both VT and LP events at almost the same time.
4) Tremors (TR): These events are generated due to degassing or to the effect of resonance produced by the disturbance of the cavities of the duct systems under the crater. This type of signal may last from a few minutes to several days.
5) Explosions (EX): These events are originated due to the change of pressure and temperature of the magma, in conditions where volatile gases and bubbles explode.
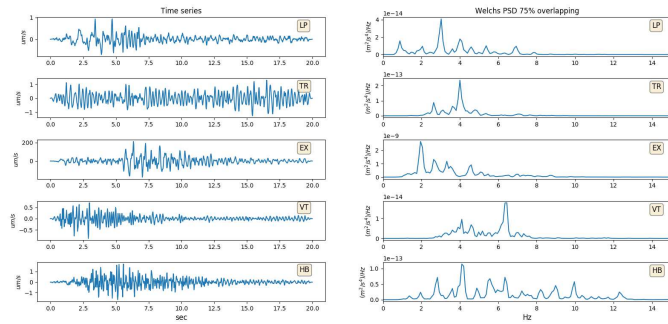
Fig. 1. Time series samples of the five classes with their respective PSD.

Our simulations showed that a temporal analysis of the seismic signals can give us important characteristics of the classes. Indeed, many time domain features have proved to be useful for distinguishing one type of signal from the others. For instance, the EX events are characterized by high magnitudes, when compared to other classes, as illustrated in Fig. 1, which shows one time series sample of each class, with their respective PSDs. In this example, it can be viewed that the maximum amplitude of the EX signal in the time domain is more than 200 um/s, while the signals of the other classes reach less than 1 um/s.

However, the simulations also showed that certain types of signals are better distinguished in the spectral domain, such as HB and VT signals. In Fig. 1, the HB and VT waveforms present a roughly similar behavior in the time domain. Nevertheless, it can be viewed that by their PSDs in Fig. 1 that the HB signal has a spectrum much broader than the VT signal, whose PSD is mainly concentrated around 6.5 Hz.

In the literature, the use of the cepstral domain has provided a relevant impact in the classification of seismic signals, e.g. [8] and [9]. Due to this fact, attributes in the cepstral domain are also considered in the proposed method. Specifically, the mel frequency cepstral coefficients (MFCC) are used in this article, as they have given good results in the classification of volcanic signals, as in [18] and [25].

C. Database

The catalog with the seismic data used in our research was built by the IGP. In the Ubinas volcano, there is a permanent seismic monitoring with four seismic stations (with codes UB1, UB2, UB3 and UB4) distributed on the flanks of the volcano, as shown in Fig. 2. From 2006 to 2007, the UB1, UB2, UB3 and UB4 stations were equipped with 1 Hz short period seismometers with an analog telemetry system for transmitting data to the observatory (IGP Arequipa). From 2008 to the present, these stations were progressively upgraded with broadband 3 component sensors and digital telemetry based on Guralp 40T and Reftek 130. The initial catalog was made mainly using the data recorded by these 4 permanent stations. However, the UB1 and UB2 stations have more stable instruments in terms of continuity of the data acquisition without gaps. Therefore, this work uses only data from the stations UB1 and UB2, located approximately 2 km to the

west and north of the crater, respectively. The database of our research was collected in the year 2014 and, at that time, the station UB1 had a 3 component sensor, while UB2 had a single component sensor. This means each event is characterized by 4 simultaneous signals in the final database.

The catalog used in this work consists of records of the five aforementioned main volcano-seismic events (VT, LP, HB, TR and EX) with the corresponding labels assigned by the experts of the IGP. There are other types of events exhibited in the literature, such as "Tornillo" (TOR), Very Long Period (VLP). However, there are not enough data found of these types of events. Due to this reason, they were not considered in this work.

The catalog is used to compare the responses of the automatic classifier with the ones of the experts, and to calculate the success rate of the classifier. Results of several temporary experiments, with other databases of seismic data collected by sensors located around the Ubinas volcano, were carried out in the years 2006, 2009, 2011, 2014 and 2015, with international participation, such as in the framework of the EU-VOLUME project [22], a cooperation between the IGP and the *Institut de Recherche pour le Developpement* (IRD-France).

Due to the considerable number of volcanic events that occurred in 2014 (about 50,000 events), this database has a high number of events cataloged. In particular, it has a considerable number of explosion events, when compared with databases of other works, which can be considered one of the most important events to be detected. For instance, the database of [18] contains only 160 EX events. Besides, our database has a continuity in the data, that is, it has no gaps in the acquisition of the signals. The complete catalog has 28140, 11489, 8108, 1346 and 592 events of the classes LP, TR, HB, VT and EX, respectively. However, in order to maintain a balance among the number of samples in each class, we decided to use a smaller number of events, as it will be described in Section IV.

III. CLASSIFICATION SYSTEM

In this section, the proposed supervised classification method is presented. Fig. 3 shows a simplified block diagram of the classification system, based on a multicomponent processing by using 4 seismic channels from 2 different stations. The classifier can be summarized in the following steps, which will be detailed in the sequel. Firstly, a signal conditioning that includes offset elimination and instrumental correction, among other operations, is performed. The extraction of the attributes in temporal, spectral and cepstral domains is then carried out, using the EMD. A simplified scheme of the feature extraction block diagram is shown in Fig. 4. After this step, the PCA and SVM techniques are applied.

A. Signal Conditioning

By analyzing the PSD of the signals of the different classes, it was found that the spectral bandwidth of interest can be considered lower than 20 Hz. Due to this reason, the sampling rate of all the signals was set to 50 Hz. In addition, the averages
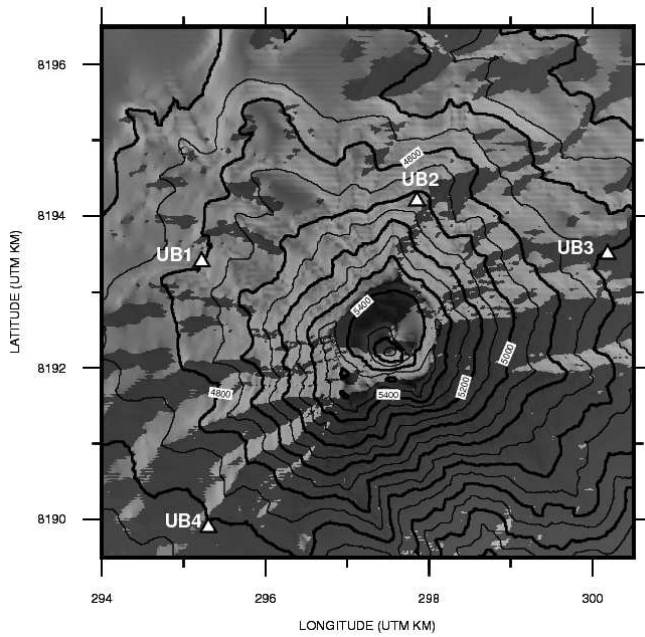
Fig. 2. Map of the Ubinas volcano with the UB1, UB2, UB3 and UB4 permanent stations.
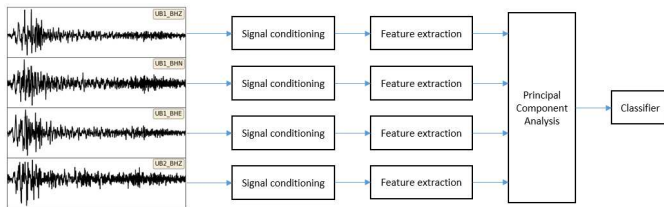

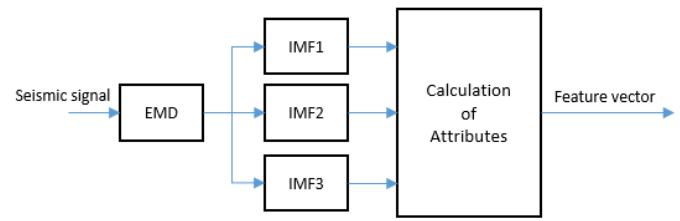Fig. 3. Simplified block diagram of the proposed classification system.

Fig. 4. Feature extraction block diagram.

Fig. 5. Simplified block scheme of the data acquisition system from the ground motion until the reception system.

of the signals were removed with the objective of avoiding low frequency artifacts in the PSD.

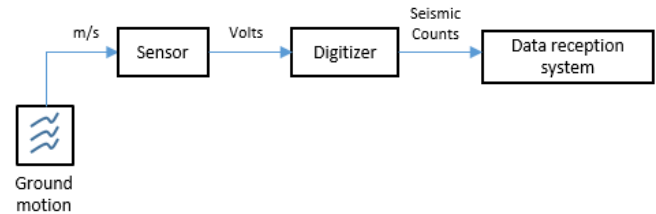The instrumental correction is then carried out, converting the data from Seismic Counts into m/s. As shown in Fig. 5, which shows a simplified block scheme of the data acquisition system from the ground motion until the reception system, the velocity signals are recorded by the digitizers of the monitoring centers in the unity Seismic Counts. The instrumental correction consists in computing the deconvolution associated with the transfer function of the data acquisition system (sensor transfer function multiplied by the digitizer sensitivity), bringing back the seismic signal to its original unity (m/s). This method for instrumental correction is detailed in [20].

The use of the instrumental correction is due to a specific reason. By standardizing all the velocity signals to the unit m/s, the classifier becomes independent of the types of sensors used. Otherwise, we would be forced to normalize the signals, as seen in some cases in the literature [18], [26]. However, when a normalization is performed, valuable information of the physical energy of the signals is lost. This is particularly important in our study, as more than one type of sensor is being used simultaneously. That gives to the energy of the signals a physical sense, allowing us to use the energy as an important attribute. In the simulation results, we have shown that the instrumental correction significantly improves the accuracy of the classifier.

An example of the importance of the instrumental correction can be viewed by comparing the LP and EX signals in Fig. 1. These signals have similar spectra, the main difference between these two signals being the high energy of the EX signal when compared to the LP. This characteristic can be reflected in attributes such as the energy or the maximum of the temporal signal. Indeed, in Fig. 1, the maximum of the LP signal is 0.94 um/s, while the EX signal has a maximum of 211.7 um/s.

B. Feature Extraction

In this subsection, the feature extraction procedure is described. A simplified scheme of the feature extraction block is shown in Fig. 4. As earlier explained, the proposed classifier is based on a multicomponent approach by using 4 seismic channels from 2 different stations, i.e. each volcano-seismic observation is represented by 4 simultaneous seismic signals: 3 signals observed by a station with a triaxial sensor (UB1) and 1 signal observed by a station with a single-channel sensor (UB2).

After the preprocessing steps described in Subsection III-A, each of the 4 signals are decomposed with the use of EMD, the 3 most significant IMFs being selected and the others being neglected. A large number of attributes is then calculated for each IMF of each signal. These steps of the feature extraction block are detailed in the sequel.

a) Empirical Mode Decomposition: The EMD is a self-adaptive filter developed by Huang in 1998 for analysis of nonlinear and non-stationary signals [19]. This method has been applied in the study of gravitational waves [27], noise analysis [28], acoustic signals [30], image processing [31], etc. The use of EMD method is relatively new in seismology. For instance, the works [21], [29], [32], [33] recently applied the EMD for this type of signal. Up to now, the use of EMD

for classification of volcano-seismic signals using machine learning was not found in the literature.

The principle of the EMD is to decompose a signal, through a sifting process, into different modes called IMFs. The term IMF is due to the fact that the EMD does not use a fixed type of basis function to compute the decomposition, as it usually happens in signal transforms, like, for instance, the Wavelet and Fourier transforms. On the contrary, the EMD performs the decomposition based on natural or intrinsic characteristics of the signal. The IMFs occupies different frequency bands, the first IMFs containing roughly high frequencies and the last ones containing roughly low frequencies. In the present article, the natural characteristics of the IMFs are exploited to generate the feature vector, in order to obtain a better representation of the different types of signals to be classified.

The steps of the EMD of a discrete-time signal $x[n]$ are illustrated in Fig. 6, with the following remarks:

- In this work, we used cubic spline to interpolate the upper envelope and lower envelopes.
- The conditions for $h_1[n]$ to be an IMF are the following:
    a) the number of extrema and the number of zero-crossing points must be equal or differ at most by one;
    b) $m_k[n]$ must be 0 at some point.
- The standard deviation (SD) is defined as:

$$SD = \sum_{k=1}^{N} \frac{|h_{k-1}[n] - h_k[n]|^2}{h_{k-1}^2[n]}. \tag{1}$$

- $I_m[n]$ is the mth IMF of $x[n]$.
- The original signal $x[n]$ can be represented as follows:

$$x[n] = \sum_{m=1}^{M} I_m[n] + r[n], \tag{2}$$

where M is the number of IMFs and $r[n]$ is the final residual signal.

b) Choice of the Number of IMFs: After computing the EMD, one must decide how many IMFs will be used for generating the attributes. Indeed, as the EMD method is a natural decomposition method, the number of IMFs is not fixed, it depends on each signal. It is then essential to fix a number of IMFs to perform the extraction of attributes. Otherwise, the number of attributes would be variable. In the present work, the Variance Contribution Ratio (VCR) is used for this purpose. The VCR represents the variance of each IMF with respect to the total variance, that is:

$$VCR_{I_m} = \frac{\text{var}(I_m[n])}{\sum_{m=1}^{M} \text{var}(I_m[n])} \tag{3}$$

where $\text{var}(\cdot)$ is the variance operator. We have calculated all the VCR_{I_m} for a sample space of 2000 events (400 events per class), obtaining as a result that the first 3 IMFs from the 3 highest VCRs provide a VCR of at least 93%, i.e. $VCR_{I_1} + VCR_{I_2} + VCR_{I_3} \geq 0.93$. This means that the sum of the remaining IMFs represents, on average, less than 7% of the total energy. These remaining IMFs can then be considered noise, which means that the first 3 IMFs together account for most of the energy of the original signal. Due to this reason,
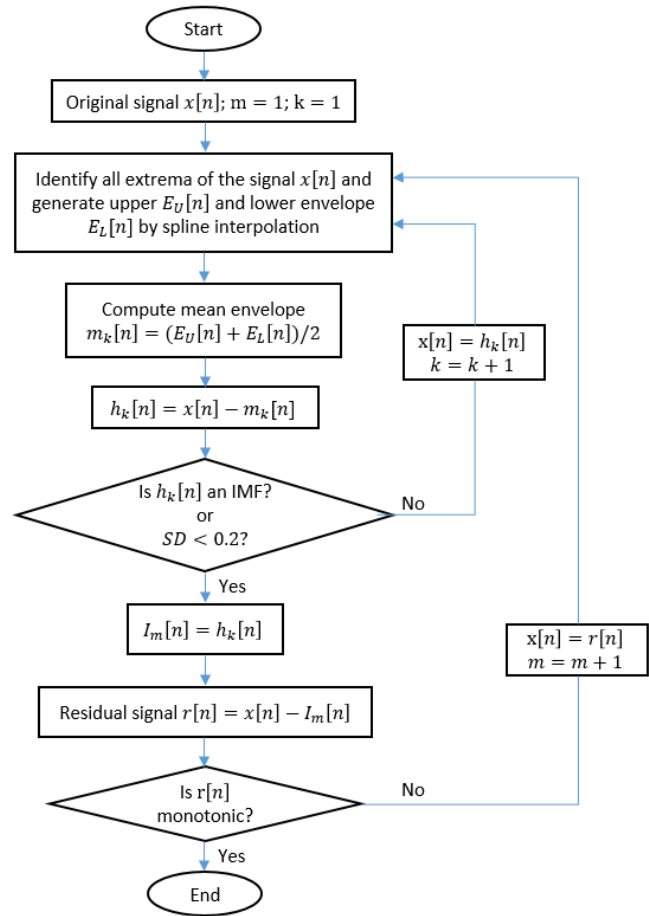

Fig. 6. Flowchart of the EMD.

we choose to use the first 3 IMFs that represent the highest amount of VCR. As a result, for each seismic event, we have 4 seismic signals, each one with 3 IMFs, leading to a total of 12 IMFs for each event.

Fig. 7 show the three selected IMFs of an LP signal, as well as their respective PSDs. It is known that a signal of the LP type has a spectrum with energy concentrated at low frequencies, generally less than 5 Hz. It can be viewed from this figure that the first IMF has a considerable energy in frequencies between 3 to 5 Hz, and each subsequent IMF has a spectrum concentrated around a lower frequency. Indeed, the second IMF has a high energy concentration around 3 Hz, and the third IMF has considerable energy around 1 and 3 Hz. From the fourth IMFs onwards, the energies are not considerably high. In comparison to the original signal, there are now 3 signals (IMFs) that reinforce that the signal is LP type. This nature of IMFs helps to differentiate between one class and another. The attributes used by the classifiers will be extracted from the 12 IMFs that represents a volcano-seismic event to take even more advantage of the natural characteristics of these signals, in order to generate a feature vector that represent efficiently each class.

c) Calculation of Attributes: As explained in Subsection II-B, our simulations showed that certain types of classes are better distinguished in the time domain, while other signals are
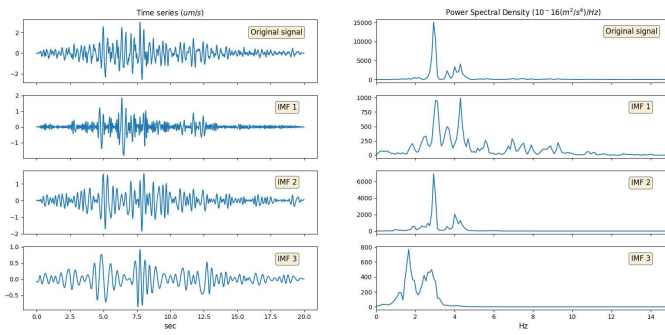
Fig. 7. A sample of an LP signal, its three selected IMFs and their PSD.

TABLE I
ATTRIBUTES EXTRACTED FROM THE IMFS

Name	Formula	s[k]
Duration	$length(s[k])/Fs$	$I_i[k]$
Zero-crossing rate	$\dfrac{count(s[k]s[k-1]<0)}{length(s[k])}$	$I_i[k]$
Maximum Energy	$max(s[k])$	$I_i^2[k]$ $PSD_k(I_i[n])$
Maximum index	$argmax(s[k])$	$I_i^2[k]$ $PSD_k(I_i[n])$
Centroid	$\dfrac{\sum_k k\,s[k]}{\sum_k s[k]}$	$I_i^2[k]$ $PSD_k(I_i[n])$
Skewness	$\dfrac{1}{length(s)}\cdot\sum_k\left(\dfrac{s[k]-mean(s)}{std(s)}\right)^3$	$\|H\{I_i[k]\}\|$ $PSD_k(I_i[n])$
Kurtosis	$\dfrac{1}{length(s)}\cdot\sum_k\left(\dfrac{s[k]-mean(s)}{std(s)}\right)^4$	$\|H\{I_i[k]\}\|$ $PSD_k(I_i[n])$
Increase vs decrease duration	$\dfrac{t_M-t_{init}}{t_{final}-t_M}$ where $\quad t_M=argmax(s[k])$	$\|H\{I_i[k]\}\|$
Maximum increment and decrement	$max(s[k]-s[k-1])$ $min(s[k]-s[k-1])$ with $\;s[k]s[k-1]<0$	$I_i^2[k]$ $PSD_k(I_i[n])$
MFCC	$s[k]$	$F_k^{-1}\{\log\|F\{I_i[n]\}\|\}$
Others	mean, standard deviation, Shannon and Renyi entropy, etc.	-

better distinguished in spectral or cepstral domains. A good success rate using the 3 aforementioned domains was obtained in [18]. Due to this reason, the proposed classification system performs the extraction of the attributes in temporal, spectral and cepstral domains, in the following way:

- In the temporal domain, we used attributes obtained directly from the IMFs $I_i[n]$.
- In the spectral domain, we used attributes calculated from the PSDs of the IMFs, using the Welch's method [34] with an FFT length of N = 512, 75% overlapping and a Hanning window function.
- In the cepstral domain, we used attributes obtained from $F^{-1}\{\log|F\{I_i[n]\}|\}$, where $F\{\cdot\}$ is the Fourier transform, with 13 Mel frequency coefficients (MFCC) being used.

A total of 54 attributes are extracted per IMF. Table I shows some of the used attributes, where $s[n]$ is the signal from which the attributes are extracted, and Fs is the sampling frequency. For time domain attributes, $s[k] = I_i[k]$, $s[k] = I_i^2[k]$ or $s[k] = |H\{I_i[k]\}|$, where $H\{\cdot\}$ is the Hilbert Transform and $|\cdot|$ the absolute value. For frequency domain attributes, $s[k] = PSD_k(I_i[n])$, where $PSD_k(\cdot)$ is the kth component of the PSD. For attributes in the cepstral domain, $s[k] = F_k^{-1}\{\log|F\{I_i[n]\}|\}$, where $F_k^{-1}\{\cdot\}$ is the kth component of the inverse Fourier transform. Moreover, the function $count(a < b)$ returns the number of components for which $a < b$.

As 12 IMFs are used per event, each seismic signal has a feature vector with $12 \times 54 = 648$ attributes. Moreover, one additional attribute was calculated directly from the raw time series: the duration of the observation. That leads to a total of 649 attributes per event. Most of these attributes were used in [18] and [35], they have proved to be useful in distinguishing signals in classification problems.

C. Principal Component Analisys (PCA)

The very high dimensionality of the above described feature vector (649 dimensions) may cause a dispersion of the data and the well-known problem of "curse of dimensionality" [36]. To avoid this issue, the PCA is used for dimensionality reduction. The use of PCA also reduces the computational complexity, improving the response time of the classifier by representing the feature vector in a smaller dimensional subspace. Moreover,

the PCA removes redundant information by using uncorrelated components.

It was found that the first 200 components obtained with PCA account for 99.7% of the feature vector variance. The number of PCA components was then set to 200, leading to a feature vector with 200 dimensions at the input of the classifier. Besides avoiding these problems, the PCA also decreases considerably the processing time, which is very important because in our case, as the proposed classification system should be able to be implemented in seismic monitoring centers in real time.

D. Classification

The last step of the proposed classification system is design a classifying algorithm, for performing the separation of the 5 classes in a space of 200 dimensions given by the PCA components. Four classification techniques were initially tested: as Multilayer Perceptron (MLP), Linear Discriminant Analysis (LDA), Random Forest (RF) and SVM. These methods have already been tested in the context of seismic events. For instance, MLP was used to classify three classes of the Stromboli volcano, in Italy [37]. The LDA was tested for classifying seismic signals with the goal of differentiating earthquakes from man-made explosions [38]. The RF was used in the classification of earthquake and non-earthquake signals [39] and the SVM was used to perform classification of volcanic events [18].

As it will be viewed in simulation results, the SVM technique provided the best results. Due to this reason, the most part of

the simulation results were generated using this method. The SVM classifier performs the separation of the classes through hyperplanes that are optimized for generating the greatest possible distance between the classes. Several simulations were carried out in order to compare different SVM kernels and penalty parameters. The best results were obtained with a radial basis function (RBF) kernel, for a Gaussian parameter of $\gamma = 0.002$, and a penalty parameter equal to $C = 10$. These parameters were used as the default configuration of the SVM.

IV. SIMULATION RESULTS

This section presents simulation results that evaluate the performance of the proposed method. The database used in the experiments is described in Subsection II-C, with 800 observations from each class, excepting the EX class that has only 592 samples, which leads to a total of 3792 samples. Hold out cross validation is used for the machine learning techniques, with 70% of data used for training and 30% for testing.

A. Multi-channel vs single-channel, and Machine Learning model choice

The first experiment carried out has the objective of comparing the performances of several classification algorithms, as well as to evaluate the impact of using multiple channels. Table II shows the success rates obtained by the proposed methodology with the MLP, LDA, RF and SVM classification techniques, for 1 and 4 channels. Many simulations were carried out to adjust some parameters of these classifiers. For the MLP, the best results were found with 2 layers, 100 neurons in the first layer and 50 in the second, and rectified linear units as activation functions. For the RF method, 750 trees provided the best success rates. For the SVM, as earlier mentioned, the best results were obtained with a RBF kernel, for a Gaussian parameter of $\gamma = 0.002$ and a penalty parameter equal to $C = 10$.

It can be viewed in Table II that, for all the tested cases, the multichannel approach provides a higher success rate than the single channel approach. The main difference between these two approaches is observed when the SVM technique is used. In this case, the use of the multiple channels improves the success rates in 7.3%. It can also be viewed in Table II that the SVM provided the best results, for both the single-channel and multi-channel cases. The best success achieved by the proposed classification system, obtained with the SVM and multiple channels, is equal to 90.5%. Due to the high success rate presented by the SVM model, this technique will be used as the training model for the next simulation results.

B. EMD performance

The next simulation results have the objective of evaluating the impact of the use of the EMD. Table III shows the confusion matrix obtained by the proposed classification system using the SVM and multiple channels, using the EMD (in parentheses) and without using the EMD. When the EMD is not used, the attributes are directly calculated from the raw time series,

TABLE II
SUCCESS RATE FOR SEVERAL CLASSIFICATION TECHNIQUES - SINGLE-CHANNEL AND MULTI-CHANNEL CASES

Classifier	Success Rate	
	Single-channel	Multi-channel
LDA	79.3%	83.6%
MLP	80.9%	84.6%
RF	80.8%	86.6%
SVM	83.2%	90.5%

using all the three aforementioned domains. Firstly, it can be concluded from this table that all the classes have balanced success classification rates, the EX and TR classes presenting the best results and the LP providing the worst performance. The best success rate is obtained by the EX class with the use of the EMD (98.8 %). This comes from the fact that the EX class can be easily distinguished from the other classes due to its high energy. On the other hand, the LP class is sometimes mistaken with the VT class.

It can also be viewed from Table III that EMD increases the success rate of 4 of the 5 classes, the LP class being the most impacted by the use of the EMD. Indeed, the success rate of the LP is improved by 4.2% when the EMD is used. In contrast, the classification rate of the HB class is slightly worse when EMD is used. This is due to the fact that the signals of the HB class share characteristics of the VT and LP classes. As the LP class has generally low-frequency components and the VT signal are characterized by high-frequency components, the HB class contains considerable energies at both high and low frequencies. As a consequence, the EMD of a HB signal has significant energy at first IMFs (high frequencies), as well as the last IMFs (low frequencies). This means that the IMFs of the HB class are often similar to those of the LP and VT classes, which may cause a classification error when a HB event occurs. This behavior is illustrated in Table III that shows a significant number of errors from the true class HB to the estimated class VT and, to a lesser extent, to estimated class LP.

Moreover, the overall success rate is improved by 1.5% when the EMD is used, compared with the case where it is not used. This means that the use of the EMD decreases the error rate from 11% to 9.5%. Although the gain provided by the EMD in the overall success rate is not very high, it should be highlighted that the EMD yielded more significant gains for LP and EX classes (2.7% and 4.2%, respectively). Indeed, the detection of these classes can be considered more relevant for the classification system, as the most violent volcanic events generally fall into the EX class, and the LP is very relevant for the forecast of eruptions [2], [40], [41].

C. Performance of instrumental correction

The next experiment evaluates the impact of the instrumental correction described in Subsection III-A. Table IV shows the confusion matrix obtained without the instrumental correction. Comparing the results of Tables III and IV, it can be viewed that the instrument correction has a great impact on the success

TABLE III
CONFUSION MATRIX WITH THE TRUE AND PREDICTED CLASSES, USING MULTIPLE CHANNELS AND SVM - WITHOUT EMD AND WITH EMD (IN PARENTHESES)

Overall (%):		True class				
89.0 (90.5)		LP	TR	EX	VT	HB
Predicted class	LP	**198 (208)**	3 (3)	0 (0)	5 (5)	4 (3)
	TR	4 (1)	**231 (232)**	0 (0)	19 (17)	2 (3)
	EX	0 (0)	0 (0)	**171 (176)**	2 (2)	3 (4)
	VT	29 (21)	0 (0)	3 (0)	**203 (205)**	21 (21)
	HB	9 (10)	6 (5)	4 (2)	11 (11)	**210 (209)**
Accuracy (%)		82.5 (86.7)	96.2 (96.7)	96.1 (98.8)	84.6 (88.0)	87.5 (87.1)

TABLE IV
CONFUSION MATRIX WITH TRUE CLASSES AND PREDICTED CLASSES, USING MULTIPLE CHANNELS AND SVM - WITHOUT INSTRUMENT CORRECTION.

		True class					
		LP	TR	EX	VT	HB	Overall
Predicted class	LP	**193**	1	1	4	0	
	TR	4	**231**	1	18	12	
	EX	1	0	**164**	0	9	
	VT	29	0	4	**199**	14	
	HB	13	7	8	19	**205**	
Accuracy(%)		80.4	96.2	92.1	82.9	85.4	87.1

TABLE V
SUCCESS RATE USING ATTRIBUTES FROM DIFFERENT DOMAINS.

Domains of the attributes	Success Rate
Temporal	81.6
Spectral	78.2
Cepstral	85.0
Temporal-Spectral	84.2
Temporal-Cepstral	87.5
Spectral-Cepstral	85.5
Temporal-Spectral-Cepstral	90.5

rate. Indeed, without the preprocessing, all the classes showed a reduction in the success rate in relation to the classification using the instrumental correction. The overall success rate falls to 87.1% without the instrument correction. This is due to the fact that, as earlier mentioned, without the signal conditioning, valuable information of the physical energy of the signals is lost. On the other hand, the instrumental correction gives to the energy of the signals a physical sense, providing valuable information.

D. Performance of the temporal, spectral and ceptral domains

The last experiment carried out evaluates the success rate when the attributes are extracted from different domains, using the SVM with the EMD and multiple channels. Table V shows the success rates obtained using seven different combinations of domains. When only one domain is used, the cepstral domain provided the best result, reaching 85.0% of success rate, and the worst performance is obtained by the spectral domain, with a success rate of 78.2%. As expected, using only one domain of attributes leads to worse success rates than using more than one domain. It can also be observed that the use of the three domains together generates the best success rate (90.5%), with a 3% gain over the second best case (temporal-cepstral), which corroborates with the use of the three domains in the proposed classification system.

V. CONCLUSIONS AND PERSPECTIVES

An automatic classification system for identifying the five most important types of events of a volcano was presented

in this paper, using the EMD in the feature extraction block. This decomposition, in conjunction with machine learning techniques, has shown to be a promising tool for classification of volcanic-seismic signals. Although the gain provided by the EMD in the overall success rate is not very high, it yielded more significant gains for the LP and EX classes, whose detection can be considered more relevant than the other classes.

Another contribution of this work is the use of multiple seismic channels to perform the classification, contrary to previous works that use only a single channel. The multi-channel approach has provided much smaller error rates when compared to the single-channel case, due to the valuable information added to the classifier. The presented system also performs an instrument correction that helps significantly in the recognition of the classes. This preprocessing standardizes the signals of the seismic sensors to their real values in m/s, making the proposed system independent of the types of sensors used and giving a physical sense to the data. Concerning the classification algorithm, four classification techniques were tested in conjunction with PCA, the SVM providing the best results.

The present investigation used a large database from the Ubinas volcano located in Arequipa, Peru. This database is particularly rich in explosion events, when compared with other volcano databases. The simulation showed a good performance of the proposed classifier, with a success rate of 90.5%.

In future works, a complexity analysis of the proposed method will be carried out, as well as some variants of the EMD might be considered, such as the Ensemble EMD (EEMD), Complete Ensemble EMD (CEEMD), among others. Moreover, the presented classification system will be implemented in real time in the volcano monitoring center of the IGP.

REFERENCES

[1] M. B. Rahman, I. S. Nurhasanah, S. P. Nugroho, "Community Resilience: Learning from Mt Merapi Eruption 2010," Procedia - Social and Behavioral Sciences, vol. 227, pp. 387-394, 2016.
[2] S. R. McNutt, "VOLCANIC SEISMOLOGY," Annual Review of Earth and Planetary Sciences, vol. 33, pp. 461-491, 2005.

[3] J. Wassermann, "Volcano Seismology," in IASPEI New manual of seismological observatory practice 2 (NMSOP-2), 2nd ed., Potsdam : Deutsches GeoForschungsZentrum GFZ, 2012, ch. 13, pp. 1-77.

[4] M. Benbrahim, K. Benjelloun, A. Ibenbrahim, M. Kasmi, E. Ardil, "A New Approaches for Seismic Signals Discrimination," International Journal of Geological and Environmental Engineering, vol. 1, pp. 64-67, 2007.

[5] J. C. Gross, J. R. R. Ritter, "Time domain classification and quantification of seismic noise in an urban environment," Geophysical Journal International, vol. 179, pp. 1213-1231, Nov. 2009.

[6] E. Yildirim, A. Gülbag, H. Gündüz, D. Emrah, "Discrimination of quarry blasts and earthquakes in the vicinity of Istanbul using soft computing techniques," Computers & Geosciences, vol. 37, pp. 1209-1217, Sep. 2011.

[7] K. V. Kislov, V. V. Gravirov, "Use of artificial neural networks for classification of noisy seismic signals," Seismic Instruments, vol. 53, pp. 87-101, Jan. 2017.

[8] Q. Zhou, G. Tong, D. Xie, B. Li, X. Yuan, "A Seismic-Based Feature Extraction Algorithm for Robust Ground Target Classification," IEEE Signal Processing Letters, vol. 19, pp. 639-642, Oct. 2012.

[9] P. Peng, Z. He, L. Wang, "Automatic Classification of Microseismic Signals Based on MFCC and GMM-HMM in Underground Mines," Shock and Vibration, vol. 2019, pp. 1-9, Jun. 2019.

[10] J. Ramirez, F. G. Meyer, "Machine Learning for Seismic Signal Processing: Phase Classification on a Manifold," 2011 10th International Conference on Machine Learning and Applications and Workshops, vol. 1, pp. 382-388, 2011.

[11] S. Scarpetta, F. Giudicepietro, E. C. Ezin, S. Petrosino, E. Del Pezzo, M. Martini, M. Marinaro, "Automatic Classification of Seismic Signals at Mt. Vesuvius Volcano, Italy, Using Neural Networks," Bulletin of the Seismological Society of America, vol. 95, pp. 185–196, Feb. 2005.

[12] G. Curilem, J. Vergara, G. Fuentealba, G. Acuña, M. Chacón, "Classification of seismic signals at Villarrica volcano (Chile) using neural networks and genetic algorithms," Journal of Volcanology and Geothermal Research, vol. 180, pp. 1-8, 2009.

[13] A. Bueno, M. Titos, L. García, I. Álvarez, J. Ibañez, C. Benítez, "Classification of Volcano-Seismic Signals with Bayesian Neural Networks," 2018 26th European Signal Processing Conference (EUSIPCO), pp. 2295-2299, Sep. 2018.

[14] M. Ohrnberger, "Continuous automatic classification of seismic signals of volcanic origin at Mt. Merapi, Java, Indonesia," Ph.D. dissertation, Faculty of Mathematics and Natural Sciences, University of Potsdam, Germany, 2001.

[15] C. Benitez, J. Ramirez, J. C. Segura, A. Rubio, J. M. Ibañez, J. Almendros, A. Garcia-Yeguas, "Continuous HMM-Based Volcano Monitoring at Deception Island, Antarctica," 2006 IEEE International Conference on Acoustics Speech and Signal Processing Proceedings, vol. 5, pp. V-749-V752, May 2006.

[16] L. Gutiérrez, J. Ibañez, G. Cortés, J. Ramírez, C. Benítez, V. Tenorio, Á. Isaac, "Volcano-seismic signal detection and classification processing using hidden Markov models. Application to San Cristóbal volcano, Nicaragua," 2009 IEEE International Geoscience and Remote Sensing Symposium, vol. 4, pp. IV-522-IV-525, 2009.

[17] W. Du, Z. Zhang, "Application of Wavelet Analysis in Seismic Data Processing of Volcanic Rock Region," 2010 International Conference on Intelligent System Design and Engineering Application, vol. 1, pp. 371-374, Oct. 2010.

[18] M. Malfante, M. Dalla-Mura, J. P. Métaxian, J. I. Mars, O. Macedo, L. A. Inza, "Machine Learning for Volcano-Seismic Signals: Challenges and Perspectives," IEEE Signal Processing Magazine, vol. 35, pp. 20-30, Mar. 2018.

[19] N. E. Huang, Z. Shen, S. R. Long, M. C. Wu, H. H. Shih, Q. Zheng, N. C. Yen, C. C. Tung, H. H. Liu, "The empirical mode decomposition and the Hilbert spectrum for nonlinear and non-stationary time series analysis," Proceedings of the Royal Society of London, vol. 454, pp. 903-995, Mar. 1998.

[20] J. Havskov, G. Alguacil, "Correction for instrument response," in Instrumentation in Earthquake Seismology, 2nd ed., Springer, 2004, ch. 6, pp. 197-215.

[21] L. A. Inza, "Understanding magmatic processes and seismo-volcano source localization with multicomponent seismic arrays," Ph.D. dissertation, Earth Sciences, Université de Grenoble, France, 2013.

[22] O. Macedo, J. P. Métaxian, E. Taipe, D. Ramos, L. A. Inza, "Seismicity associated with the 2006-2008 eruption, Ubinas volcano," The VOLUME Project, pp. 262-270, 2009.

[23] L. A. Inza, J. P. Métaxian, J.I. Mars, C.J. Bean, G. S. O'Brien, O. Macedo, D. Zandomeneghi, "Analysis of dynamics of vulcanian activity of Ubinas volcano, using multicomponent seismic antennas," Journal of Volcanology and Geothermal Research, vol. 270, pp. 35-52, Jan. 2014.

[24] L. A. Inza, J. I. Mars, J. P. Métaxian, G. S. O'Brien, O. Macedo, "Seismo-volcano source localization with triaxial broad-band seismic array," Geophys Journal International, pp.371-384, 2011.

[25] M. C. Benitez, J. Ramirez, J. C. Segura, J. M. Ibanez, J. Almendros, A. Garcia-Yeguas, G. Cortes, "Continuous HMM-Based Seismic-Event Classification at Deception Island, Antarctica," IEEE Transactions on Geoscience and Remote Sensing, vol. 45, pp. 138-146, Jan. 2007.

[26] R. L. Cueva, V. P. Salazar, M. V. Chaluisa, "Towards an Automatic Detection System of Signals at Cotopaxi Volcano," Dyna, vol. 84, pp. 176-184, 2017.

[27] J. B. Camp, J. K. Cannizzo, K. Numata, "Application of the Hilbert-Huang Transform to the Search for Gravitational Waves," PHYS REV D, Jan. 2007.

[28] A. Komaty, A. Boudraa, D. Dare, "EMD-based filtering using the Hausdorff distance," 2012 IEEE International Symposium on Signal Processing and Information Technology (ISSPIT), Dec. 2012.

[29] R. Han, J. Li, G. Cui, X. Wang, W. Wang, X. Li, "Seismic Signal Detection Algorithm Based on GS Transform Filtering and EMD Denoising," 2018 IEEE 4th International Conference on Computer and Communications (ICCC), pp. 1213-1217, Dec. 2018.

[30] V. Grulier, S. Debert, J. I. Mars, M. Pachebat, "Acoustic and turbulent wavenumbers separation in wall pressure array signals using EMD in spatial domain," 2008 IEEE International Conference on Acoustics, Speech and Signal Processing, pp. 333-336, 2008.

[31] J. Nunes, E. Deléchelle, "Empirical Mode Decomposition: Applications on signal and image processing," Advances in Adaptive Data Analysis, vol. 01, pp. 125-175, 2009.

[32] B. S. Saeed, "De-noising seismic data by Empirical Mode Decomposition," Ph.D. dissertation, Department of Geosciences, University of Oslo, Norway, 2011.

[33] J. Han, "Empirical Mode Decomposition for Seismic Aplications," Ph.D. dissertation, Department of Physics, University of Alberta, Canada, 2014.

[34] K. K. Parhi, M. Ayinala, "Low-Complexity Welch Power Spectral Density Computation," IEEE Transactions on Circuits and Systems I: Regular Papers, vol. 61, pp. 172-182, Jan. 2014.

[35] S. Astapov, "Feature extraction from band-limited signals and classification of features," M. S. thesis, Faculty of Information Technology, Tallinn University of Technology, Estonia, 2011.

[36] X. Wang, I. H. Sloan, "Brownian bridge and principal component analysis: towards removing the curse of dimensionality," IMA Journal of Numerical Analysis, vol. 27, pp. 631-654, Oct. 2007.

[37] F. Giacco, A. M. Esposito, S. Scarpetta, F. Giudicepietro, M. Marinaro, "Support Vector Machines and MLP for automatic classification of seismic signals at Stromboli volcano," Proceedings of the 2009 Conference on Neural Nets WIRN 2009, pp. 116-123, 2009.

[38] O. Lindenbaum, Y. Bregman, N. Rabin, A. Averbuch, "Multiview Kernels for Low-Dimensional Modeling of Seismic Events," IEEE Transactions on Geoscience and Remote Sensing, vol. 56, pp. 3300-3310, Feb. 2018.

[39] W. Li, N. Nakshatra, N. Narvekar, N. Raut, B. Sirkeci, J. Gao, "Seismic Data Classification Using Machine Learning," 2018 IEEE Fourth International Conference on Big Data Computing Service and Applications, Mar. 2018.

[40] B. A. Chouet, "Long-period volcano seismicity: its source and use in eruption forecasting," Nature, vol. 380, pp. 309-316, 1996.

[41] K. Aki, V. Ferrazzini, "Seismic monitoring and modeling of an active volcano for prediction," Journal of Geophysical Research: Solid Earth, vol. 105, pp. 16617-16640, 2000.

Pablo E. Lara (pablolr_64@hotmail.com) was born in Lima, Peru, in 1989. He received his B.Sc. and Engineer Degree from the Universidad Nacional de Ingenieria (UNI) in Lima, Peru, in 2014 and 2017, respectively. In 2019, he received his M.Sc. degree in Electrical Engineering and Computer Science from the Universidade Federal do Ceara (UFC), Sobral, Brazil. His research interest lies in the area of Artificial Intelligence (AI) applied to geophysics, such as volcano seismology and earthquakes, as well as early warning systems based on AI. He is currently a researcher in Artificial Intelligence at Instituto Geofisico del Peru (IGP). He is a member of the IEEE.

C. Alexandre R. Fernandes (alexandrefernandes@ufc.br) was born in Fortaleza, Brazil, in 1981. He received the B.Sc. degree in electrical engineering from the Universidade Federal do Ceara (UFC), Brazil, in 2003, two M.Sc. degrees, from the UFC and University of Nice Sophia-Antipolis (UNSA), France, in 2005, and the double Ph.D. degree from the UFC and UNSA, in 2009, in signal processing. In 2008 and 2009, he was Teaching Assistant with the UNSA/FR and, from July 2009 to February 2010, he was a Postdoctoral Fellow with the Department of Teleinformatics Engineering, UFC. In 2010, he joined the UFC, where he works as a Full Professor with the Department of Computer Engineering, in Sobral. His research interest lies in the area of machine learning, tensor decompositions, multilinear algebra, signal processing for communications, nonlinear systems, etc.

Adolfo Inza (ainzac@gmail.com) received his B.Sc. and Engineer Degree in Electronics Engineering from the Universidad Nacional de Ingeneria (UNI) in Lima, Peru, in 1992 and 2007 respectively. In 2009, he obtained the M.Sc. degree in Signal Processing from the Grenoble-INP, France, In 2013 he obtained his Ph.D. degree in Earth Science from the Grenoble Alpes University, France. He was enrolled at Instituto Geofísico del Peru (IGP) from 1999, focused in geophysics instruments and seismic monitoring. His research focuses on volcano seismology and early warning systems as a senior scientific researcher at IGP.

Jérôme I. Mars (jerome.mars@gipsa-lab.grenoble-inp.fr) was born in 1962. He received his Master's degree (1986) in Mechanics and Geophysics from University Joseph Fourier (currently University Grenoble Alpes) and Ph.D. degree in Signal Processing (1988) from the Institut National Polytechnique de Grenoble. He has been with CEPHAG (Centre des Phénomènes Aléatoires et Geophysiques de Grenoble) between 1989-1992, with MSME (Materials Sciences and Mineral Engineering) department, University of California, Berkeley, between 1992-1995, and with LIS laboratory (Laboratory of Images and Signal) between 1995-2007.

He is Professor with the Grenoble Institute of Technology, France. He is currently the head of the Grenoble Images Speech Signals and Automatics Laboratory. His research interests cover statistical signal processing and source separation with antennas. In particular his latest research works mostly focus in the field of wave propagation (underwater acoustics, geosciences and tomography). He is a member of the IEEE.

Jean-Philippe Métaxian (metaxian@ipgp.fr) received his master's degree in mechanics and geophysics in 1990 from University Joseph Fourier (now known as the University Grenoble Alpes), Grenoble, France, and his Ph.D. degree in geophysics in 1994 from the Université de Savoie, Chambéry, France. He has been a researcher at the Institut de Recherche pour le Développement (IRD) since 1994. He is part of the geophysics of volcanoes team at the Institut des Sciences de la Terre Laboratory and the seismology team at the Institut de Physique du Globe de Paris. His research interests include volcano seismology, and his latest focus is in the fields of volcano structure and the study of eruptive processes by using technics of dense and short aperture seismic arrays.

Mauro Dalla Mura (mauro.dalla-mura@gipsa-lab.grenoble-inp.fr) received the B.Sc. and M.Sc. degrees in Telecommunication Engineering from the University of Trento, Italy in 2005 and 2007, respectively. He obtained in 2011 a joint Ph.D. degree in Information and Communication Technologies (Telecommunications Area) from the University of Trento, Italy and in Electrical and Computer Engineering from the University of Iceland, Iceland.

He is currently an Assistant Professor at Grenoble Institute of Technology (Grenoble INP), France since 2012. He is conducting his research at the Grenoble Images Speech Signals and Automatics Laboratory (GIPSA-Lab). Dr. Dalla Mura has been appointed "Specially Appointed Associate Professor" at the School of Computing, Tokyo Institute of Technology, Japan for 2019-2022. His main research activities are in the fields of remote sensing, image processing and pattern recognition. In particular, his interests include multispectral and hyperspectral image processing, computational imaging and the analysis of geophysical signals.

Dr. Dalla Mura was the recipient of the IEEE GRSS Second Prize in the Student Paper Competition of the 2011 IEEE IGARSS 2011 and co-recipient of the Best Paper Award of the International Journal of Image and Data Fusion for the year 2012-2013 and the Symposium Paper Award for IEEE IGARSS 2014. Dr. Dalla Mura is the President of the IEEE GRSS French Chapter since 2016 (he previously served as Secretary 2013-2016). In 2017 the IEEE GRSS French Chapter was the recipient of the IEEE GRSS Chapter Award and the "Chapter of the year 2017" from the IEEE French Section. He is on the Editorial Board of the IEEE Journal of Selected Topics in Applied Earth Observations and Remote Sensing (J-STARS) since 2016.

Marielle Malfante (marielle.malffante@cea.fr) received her M.Sc. degree in Signal Processing in 2015 from Grenoble Institute of Technology, France. She then received a Ph.D. degree in Machine Learning from University Grenoble Alpes, France, for her work on Automatic Classification of Natural Signals for Environmental Monitoring. She received the First Prize Best Student Paper Award in animal bioacoustics at the Salt Lake City meeting og the Acoustical Society of America in 2016. She is currently a researcher in Artificial Intelligence at CEA, France.